Beyond Planar: An Additively Manufactured, Origami-Inspired Shape-Changing, and RFIC-Based Phased Array for Near-Limitless Radiation Pattern Reconfigurability in 5G/mm-Wave Applications

Hani Al Jamal, *Graduate Student Member, IEEE*, Chenhao Hu, *Graduate Student Member, IEEE*, Nathan Wille, Kai Zeng, *Member, IEEE*, and Manos M. Tentzeris, *Fellow, IEEE*

***Abstract*— This letter presents an origami-inspired phased array operating at 28 GHz, with on-structure beamformer RFICs and a flexible feeding network that utilizes a foldable hinge interconnect. The mm-wave origami phased array therein operates at a substantially smaller scale compared with prior literature and achieves remarkable integration with on-structure beamforming circuitry. It introduces the first additively manufactured fully foldable hinge interconnect, exhibiting near-constant insertion loss across various folding angles and cycles. Leveraging origami principles, the phased array offers near 360° continuous beam steering in the azimuth plane with reconfigurable multibeam or quasi-isotropic radiation patterns. Additive manufacturing techniques, including 3-D and inkjet printing, are used to fabricate a low-cost and lightweight prototype. Measurements demonstrating near-limitless pattern reconfigurability due to mechanical shape change and electrical beam steering signify a significant leap in overcoming challenges faced by traditional phased arrays.**

***Index Terms*— 5G, additive manufacturing, beamformer IC, mm-wave, origami, phased array.**

I. Introduction

THE landscape of high-speed communications has undergone a revolutionary shift with the introduction of 5G mm-wave technology, unlocking unprecedented potentials for the development of smart cities, industry 4.0, and consumer focused IoT through broadband and ultrareliable low-latency communication. Nevertheless, the realization of the full potential of 5G mm-wave applications faces challenges, particularly because of the effectiveness of mm-wave signals, which experience significant deterioration in non-line-of-sight conditions due to the high path loss incurred. As such, the utilization of phased arrays has become imperative to 5G deployment, offering beam-steering capabilities that can reduce interference by the direct targeting of users. Traditional phased arrays, however, grapple with inherent limitations, primarily with their limited angular coverage and narrow beamwidths. Moreover, the bulkiness, cost, and rigidity of these systems hinder adaptability, making modification or replacement of subsystem components a formidable task.

Recognizing the constraints of planar phased arrays, a promising avenue emerges with the exploration of shape-changing and multifaceted arrays. Modifying the shape of an array results in a change in the orientation and relative positioning of its elements, causing alterations in element couplings, port impedances, and resulting radiation patterns. This transformation effectively renders a distinct array for every shape configuration, enabling the utilization of the optimal array shape for a given application scenario.

Leveraging principles from origami, the art of paper folding, reconfigurable shape-changing RF structures, and antennas have been demonstrated in the literature. Origami tessellations, notably the miura-ori [1] and the "eggbox" [2], have found applications in frequency-selective surfaces (FSS), showcasing spatial frequency reconfigurability. The simplicity of fabricating these structures lies in the straightforward patterning of conductive traces. Origami antennas, spanning diverse materials, such as paper [3], PET [4], and 3-D-printed substrates [5], have demonstrated frequency reconfigurability up to 4.45 GHz. Reconfigurability in antenna radiation pattern due to shape change has been less prominent in the literature but has been presented at 2.2 GHz using a quasi-Yagi helical

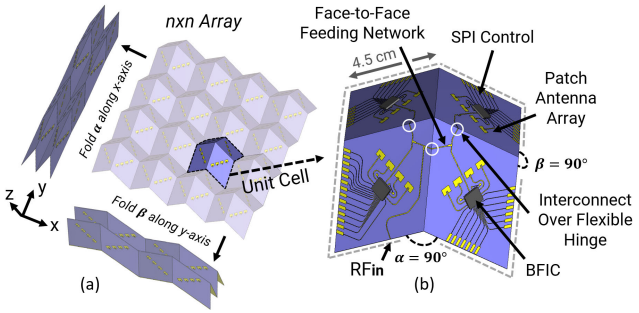

Fig. 1. (a) $n \times n$ origami-inspired eggbox antenna array with folding action along the x- and y-axes. (b) Proposed single unit cell with a geometrically optimized face-to-face feeding network and integration of four BFICs.

Manuscript received 27 April 2024; accepted 28 April 2024. Date of publication 16 May 2024; date of current version 7 June 2024. This work was supported in part by the Office of the Under Secretary of Defense (OUSD) (R&E) through Naval Information Warfare Center under Contract N6523622C8018 and in part by the Air Force Office of Scientific Research (AFOSR) under Grant FA9550-18-1-0191. *(Chenhao Hu and Nathan Wille contributed equally to this work.) (Corresponding author: Hani Al Jamal.)*

Hani Al Jamal, Chenhao Hu, Nathan Wille, and Manos M. Tentzeris are with the School of Electrical and Computer Engineering, Georgia Institute of Technology, Atlanta, GA 30332 USA (e-mail: hani.aljamal@ieee.org).

Kai Zeng is with the Department of Electrical and Computer Engineering, Cyber Security Engineering and the Department of Computer Science, George Mason University, Fairfax, VA 22030 USA.

This article was presented at the IEEE MTT-S International Microwave Symposium (IMS 2024), Washington, DC, USA, June 16–21, 2024.

Color versions of one or more figures in this letter are available at https://doi.org/10.1109/LMWT.2024.3396026.

Digital Object Identifier 10.1109/LMWT.2024.3396026

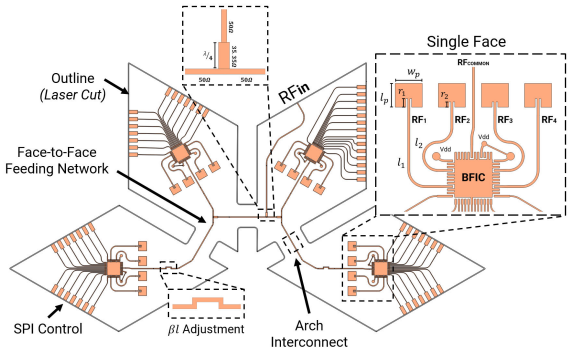

Fig. 2. Two-Dimensional mapped layout of the proposed eggbox antenna array.

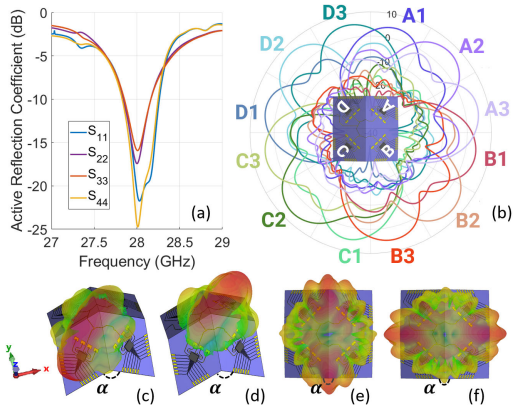

Fig. 3. (a) Simulated active reflection coefficient. (b) Simulated electronic beam steering using BFICs A–D on each eggbox face and using three BFIC configurations. (c) and (d) Simulated radiation pattern of a single face activation beaming at boresight. (e) and (f) Four face activation beaming in a desired direction; $\alpha = 90°$.

antenna [4]. In addition, Seiler et al. [6] investigate an origami-inspired *antenna array* featuring up to four patch elements at 3 GHz. However, challenges surfaced as connecting interconnects extended over folds, impacting performance with changing folding angles. Notably, this array lacked the beam-steering capabilities inherent in phased arrays, behaving more akin to a single antenna, driving Williams et al. [7] to develop an origami-inspired *phased array* at 2.6 GHz, and boasting an array of 3-by-5 elements. While demonstrating the ability to morph into planar, cylindrical, and circular geometries, this structure encounters limitations in terms of size, bulkiness, and scalability, posing challenges to its practical implementation. Designed for 2.6-GHz operation, the work in [7] is not suitable for mm-wave applications, is not additively manufactured, and does not present foldable hinge interconnects for higher integration levels and scalability.

To the best of the authors' knowledge, this letter presents the first origami-inspired phased array operating at 28 GHz with on-structure integrated beamformer ICs and a face-to-face feeding network connecting all four faces of the utilized eggbox origami, enabled by reliably foldable "arch" hinge interconnects for stable mm-wave performance (Fig. 1). While operating at 28 GHz renders the structure therein at a completely different, much smaller scale than any origami phased array previously presented in the literature, it also brings the challenge of high integration levels with the beamforming circuitry. The eggbox origami structure utilized therein is foldable along two planes and multifaceted, allowing for near 360° beam steering in the azimuth plane with multibeam patterns. A prototype is additively manufactured in Section III-B, and measurements in Section IV demonstrate the exploration of radiation pattern reconfigurability through two degrees of freedom (2-DOF), offering simultaneous electrical beam steering and mechanical shape-change adaptability, a previously unexplored dimension. Moreover, the modular tile-based approach allows for the selective activation of individual unit cells based on desired patterns, TX/RX modes, and/or power consumption requirements, paving the way for active transmit–receive relay systems, and simplified maintenance.

II. Eggbox Phased Array Unit-Cell Design

The 2-D mapped layout of the proposed unit cell is shown in Fig. 2 and consists of four individually controlled faces. Each face consists of a linear four-element patch antenna array, controlled by an AWMF-0108 beamformer RFIC through a serial peripheral interface (SPI). The AWMF-0108 is a 28-GHz quad-core IC supporting four radiating elements and TX/RX half-duplex operation, with integrated amplifiers and phase shifters capable of providing phase increments of 11.25°. The patch antenna elements are designed at 28 GHz in CST Microwave Studio on the 3-D eggbox structure in its natural unfolded state, as shown in Fig. 1. The elements are inset-fed and placed half a wavelength apart to provide the largest steerable beam angle range while avoiding grating lobes. They have the dimensions of $l_p = 2.95$ mm, $w_p = 3.37$ mm, $r_1 = 1.07$ mm, and $r_2 = 0.65$ mm, which take mutual coupling effects into account.

The four beamformer ICs (BFICs) on each face are fed by a single RF input (or output) through a face-to-face feeding network. The dynamic 3-D morphology of the origami structure, in addition to the fact that unit-cell faces are to be connected over foldable hinges, adds to the complexity of the design and prohibits a symmetric feeding network. Nevertheless, the four branches of the face-to-face feeding network are tuned to yield near-identical transmission, and "U-shaped" structures are incorporated within two branches providing an additional electrical length tuning knob. The face-to-face feeding network was measured separately and found to have at most 0.8 dB and 15° of magnitude and phase deviation between any two ports, respectively. This small deviation is compensated for using the beamformer ICs.

The simulated active reflection coefficients as seen by a beamformer IC are shown in Fig. 3(a) for the four elements excited with the required phases to radiate simultaneously, producing a beam at boresight. This phase takes into account the needed phase compensation due to not only the face-to-face feeding network but also the different transmission lines lengths connecting the BFIC to the patch elements. Moreover, the total efficiency of the elements is found to be −2.36 dB at the frequency of resonance.

Fig. 3(b) shows the simulated radiation pattern of nine individual beams overlaid in the azimuth plane, illustrating one possibility of operating the eggbox phased array: the beam from one face is phase steered to a maximum value at which the adjacent face takes over ensuring a continuous 360° angular coverage. The radiation pattern with only BFIC "C" activated in phase configuration "C2" and only BFIC "A" activated in phase configuration "A2" is shown in a 3-D space in Fig. 3(c) and (d), respectively. Activating all four BFICs and exciting the 16 patch elements with signals of appropriate phases yield the patterns of Fig. 3(e) and (f).

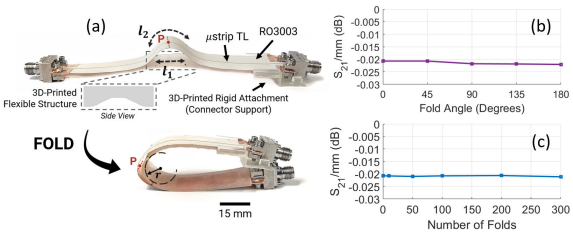

Fig. 4. (a) Proposed "arch" interconnect topology. Measured transmission coefficient for different (b) fold angles and (c) bend cycles at 28 GHz.

III. Fabrication

A. Fully Foldable mm-Wave Hinge Interconnect

As aforementioned, the designed face-to-face feeding network extends over foldable hinges required to realize the eggbox origami. While efforts have been directed at designing flexible [8] and stretchable [9] additively manufactured interconnects, it is imperative to note that these efforts differ from the challenge of fully bending interconnects over a small radius ($r \leq 2$ mm) due to the high levels of applied tensile and compressive stresses. The absence of a robust solution to this specific bending requirement has, until now, hindered the realization of fully contained origami structures at this scale and at mm-wave frequencies. Our proposed foldable "arch" hinge interconnect [Fig. 4(a)] successfully addresses this challenge. The stack up consists of a flexible 3-D printed hinge for mechanical support and a flexible RO3003 substrate (130 μm thick) onto which a 50-Ω transmission line is inkjet-printed using the fabrication process detailed in Section III-B. The flexible substrate is arched upward in the unfolded state, reducing the stresses exerted on the interconnect when folded. Essentially, the interconnect's midpoint, denoted as "P," experiences no stress. This allows for repeated folds without observing any cracks or a change in resistance and RF performance. Measurements validate near identical performance for different bend angles [Fig. 4(b)], and no degradation in performance up till at least 300 folds [Fig. 4(c)] with S_{21} remaining near constant at −0.02 dB/mm for all folding angles between 0° and 180° and throughout 24–32 GHz.

B. Additively Manufactured Origami Phased Array

The fabrication process for the proposed eggbox phased array involves a streamlined three-stage approach. First, the origami eggbox structure is designed in a 3-D CAD software, implementing mathematical formulations as outlined in [2] and incorporating the proposed hinge structure discussed in Section III-A. An origami unit cell is then 3-D printed using a Formlabs Form 3+ stereolithography (SLA) printer, utilizing flexible80A, a flexible photopolymer resin. The orientation during 3-D printing was found to be crucial, impacting hinge flexibility. To solidify the material, the printed structure undergoes sonication in an IPA bath for 20 min, followed by a 15-min UV curing treatment.

Moving to the second stage, the radiating elements and beamformer RFICs are integrated. The patch elements and RF circuitry are inkjet-printed onto an RO3003 substrate, with $\varepsilon_r = 3.0$, $\tan\delta = 0.001$, and a thickness of $h = 130$ μm. The inkjet printing involves depositing six layers of SU-8 photoresist ink using the Dimatix DMP-2831 inkjet printer. The resulting pattern is cured with a UV crosslinker, followed by copper etching in ferric chloride. A 3×3 via array, having 0.2 mm via hole diameters, is then drilled onto each BFIC's ground pad for thermal management, with the holes

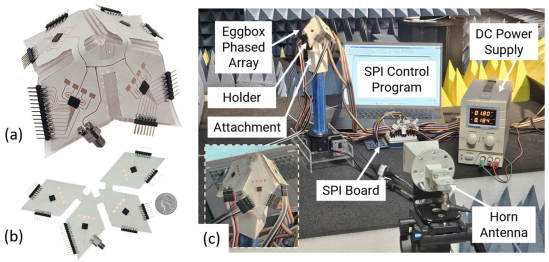

Fig. 5. Fabricated prototypes: (a) assembled unit cell on a 3-D printed flexible structure and (b) inkjet-printed eggbox phased array. (c) Measurement setup.

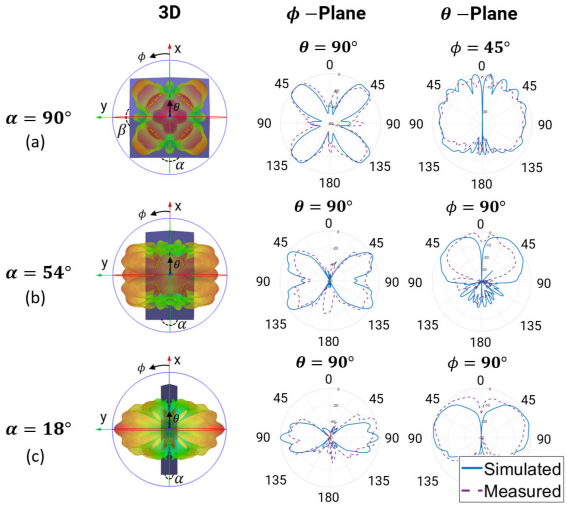

Fig. 6. Simulated and measured normalized radiation patterns for eggbox mechanical bend angles of (a) $\alpha = 90°$, (b) $\alpha = 54°$, and (c) $\alpha = 18°$.

subsequently filled with silver paste (LPKF ProConduct, $\rho = 9.42 \times 10^{-6}$ Ωm). The substrate undergoes thermal sintering at 160 °C for 30 min. Solder paste is applied to all pads, and a heat gun is utilized for solder reflow to attach the four 6×6 mm QFN packaged beamformer ICs. Header pins are soldered to provide access to the biasing and SPI control lines.

In the final assembly stage, the substrate with integrated beamformer ICs is affixed onto the flexible 3-D printed origami structure using an adhesive, as shown in Fig. 5(a) and (b). The resulting eggbox phased array, weighing 44 g and occupying a maximum volume of 6.36 cm^3 in its natural unfolded state, exemplifies the success of this fully contained, lightweight, and compact prototype achieved through additive manufacturing.

IV. Measurements

The radiation patterns of the fabricated prototype are measured in an anechoic chamber [Fig. 5(c)] for different eggbox bend angles (mechanical reconfigurability) and beamformer IC configurations (electrical reconfigurability). Initially, the beamformer ICs are configured, such that each planar face would beam at boresight. Measurements are taken in two plane cuts, and in each plane, the cross-polarization and copolarization patterns are measured, with the resulting normalized absolute patterns plotted against the simulated patterns in Fig. 6 and showing great agreement. Folding the eggbox phased array along the x-axis (decreasing α) enables a seamless transition in the radiation pattern, transforming it from four independent beams [Fig. 6(a)] to a quasi-isotropic pattern [Fig. 6(b)] and finally to two beams along the y-axis [Fig. 6(c)]. By folding along the y-axis instead, symmetrical patterns can be achieved. For a given bend angle, the position

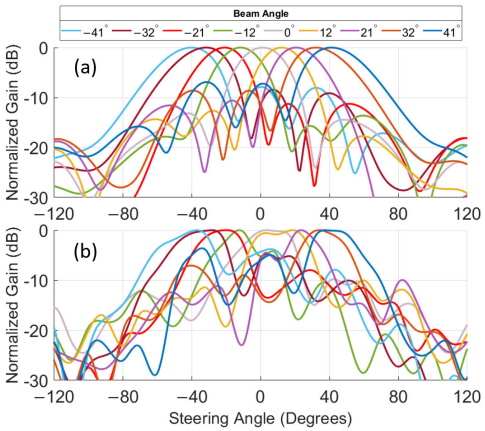

Fig. 7. (a) Simulated. (b) Measured electronic beam-steering capability.

of the pattern's nulls, beamwidth, and gain can then be independently controlled by providing the right phase conditions to the 16 radiating elements using the beamformer ICs.

Next, a single eggbox face is selectively activated to demonstrate the beam-steering capability. The steering range is simulated [Fig. 7(a)] and measured [Fig. 7(b)] at 28 GHz, and good agreement is shown. The steering angle was found to reach $\pm 41^\circ$ with a sidelobe level (SLL) reaching -7.0 dB (simulated) or -4.2 dB (measured) at worst. An increase in the measured SLL can be explained as a result of fabrication tolerances and the presence of a large number of cables for digital control. In general, increasing the number of radiating elements would decrease the SLL, in addition to decreasing the beamwidth and, as a result, increasing directivity. Amplitude tapering can also be applied to improve the performance. A slight asymmetry in the measured results can be explained by measurement errors, such as a slight misalignment between the horn antenna and eggbox phased array, which is manually carried out. The measured gain of a single four-element eggbox face is 5.6 dB at boresight and reaches 9.6 dB if the beamformer IC is utilized for amplification.

V. Conclusion

This letter presents an origami-inspired eggbox phased array operating at 28 GHz, effectively addressing the limitations of conventional planar arrays and prior origami-inspired designs. Realized through a streamlined additively manufactured process, the proposed origami phased array showcases unparalleled capabilities in radiation pattern reconfigurability, utilizing 2-DOF mechanical shape change and electrical beam steering. Our demonstration of a fully foldable hinge interconnect with minimal performance variation represents a significant advancement in compact 4-D and morphing RF structures, opening doors for realizing highly integrated shape-changing RF structures through additive manufacturing. Moreover, the multifaceted array presented therein demonstrates scalability to multiple unit cells leading to a significant increase in beam-steering precision and gain, expanded coverage angles, and additional radiation pattern reconfigurations, presenting opportunities for massive MIMO systems required for the deployment of diverse 5G/mm-wave applications.

Acknowledgment

The views and conclusions contained in this document are those of the authors and should not be interpreted as representing the official policies, either expressed or implied, of the Naval Information Warfare Center or the U.S. Government. The U.S. Government is authorized to reproduce and distribute reprints for Government purposes notwithstanding any copyright notation herein.

References

[1] Y. Cui, S. A. Nauroze, R. Bahr, and M. M. Tentzeris, "A novel additively 4D printed origami-inspired tunable multi-layer frequency selective surface for mm-Wave IoT, RFID, WSN, 5G, and smart city applications," in *IEEE MTT-S Int. Microw. Symp. Dig.*, Jun. 2021, pp. 86–89.

[2] Y. Cui, R. Bahr, S. V. Rijs, and M. Tentzeris, "A novel 4-DOF wide-range tunable frequency selective surface using an origami 'eggbox' structure," *Int. J. Microw. Wireless Technol.*, vol. 13, no. 7, pp. 727–733, Sep. 2021.

[3] X. Liu, S. Yao, N. Russo, and S. Georgakopoulos, "Tri-band reconfigurable origami helical array," in *Proc. IEEE Int. Symp. Antennas Propag. USNC/URSI Nat. Radio Sci. Meeting*, Jul. 2018, pp. 1231–1232.

[4] S. I. H. Shah, S. Gosh, M. M. Tentzeris, and S. Lim, "A novel bio inspired pattern reconfigurable quasi-Yagi helical antenna using origami DNA," in *Proc. Int. Symp. Antennas Propag. (ISAP)*, Oct. 2018, pp. 1–2.

[5] W. Su, R. Bahr, S. A. Nauroze, and M. M. Tentzeris, "Novel 3D-printed 'Chinese fan' bow-tie antennas for origami/shape-changing configurations," in *Proc. IEEE Int. Symp. Antennas Propag. USNC/URSI Nat. Radio Sci. Meeting*, Jul. 2017, pp. 1245–1246.

[6] S. R. Seiler et al., "Physical reconfiguration of an origami-inspired deployable microstrip patch antenna array," in *Proc. IEEE Int. Symp. Antennas Propag. USNC/URSI Nat. Radio Sci. Meeting*, Jul. 2017, pp. 2359–2360.

[7] D. E. Williams, C. Dorn, S. Pellegrino, and A. Hajimiri, "Origami-inspired shape-changing phased array," in *Proc. 50th Eur. Microw. Conf. (EuMC)*, Jan. 2021, pp. 344–347.

[8] J. Vaithilingam et al., "3D-inkjet printing of flexible and stretchable electronics," in *Proc. 26th Int. Solid Freeform Fabr. Symp.* Austin, TX, USA: Univ. Texas at Austin, 2015, pp. 1513–1526.

[9] T. Liimatta, E. Halonen, H. Sillanpää, J. Niittynen, and M. Mäntysalo, "Inkjet printing in manufacturing of stretchable interconnects," in *Proc. IEEE 64th Electron. Compon. Technol. Conf. (ECTC)*, May 2014, pp. 151–156.